Turkish Journal of Electrical Engineering & Computer Sciences

http://journals.tubitak.gov.tr/elektrik/

Research Article

Turk J Elec Eng & Comp Sci
(2020) 28: 621 – 634
© TÜBİTAK
doi:10.3906/elk-1904-30

Cooperative communications with optimal harvesting duration for Nakagami fading channels

Nadhir BEN HALIMA[1,*], **Hatem BOUJEMAA**[2]
[1]College of Computer Science and Engineering, Taibah University, Medina , Saudi Arabia
[2]SUPCOM, COSIM Lab. Tunisia

Received: 03.04.2019 • **Accepted/Published Online:** 16.01.2020 • **Final Version:** 28.03.2020

Abstract: In this paper, we analyze the throughput of cooperative communications with wireless energy harvesting. Relay nodes harvest energy from Radio Frequency (RF) signal transmitted by the source. We derive the packet error probability as well as the throughput for Nakagami fading channels. We also suggest to enhance the throughput by choosing the value of harvesting duration. Our results are valid for both Amplify and Forward (AF) and Decode and Forward (DF) relaying.

Key words: Energy harvesting, relaying techniques, AF and DF relaying.

1. Introduction

In cooperative systems, relay nodes help the source to deliver data to the destination. AF and DF relaying can be used to benefit from cooperative diversity. In order to reduce power consumption, relay nodes can harvest energy from RF signal transmitted by the source S [1-4]. Other source of power can be used such as wind or solar. Different relay selection techniques can be implemented for Energy Harvesting (EH) systems such as opportunistic relaying [5-7]. In opportunistic AF relaying, the chosen relay has the largest Signal to Noise Ratio (SNR). In opportunistic DF, the chosen relay offers the highest SNR of second hop and is selected between relays having correctly decoded the source packet [5-7]. The EH for two-way relaying has been suggested in [8-9]. In two-way relaying, transmission is performed from one node N_1 to a node N_2 in both directions and at the same time through a relay. Node N_1 will suppress its own signal to decode that of N_2. Also, N_2 will suppress its signal before decoding that of node N_2. EH with optimal power allocation has been suggested in [10-12]. The EH for multiantenna systems has been suggested in [13-14] to benefit from spatial diversity since the best antenna can be activated. EH for cognitive radio has been studied in [15-17]. In such systems, primary and secondary harvest energy from RF signals and share the same spectrum. The secrecy outage probability of EH systems has been analyzed in [18-21]. In such a system, there are a source, some relays, a destination and an eavesdropper trying to decode the source message.

In [1-21], harvesting duration has not been optimized. In [22], the throughput has been maximized by optimizing harvesting duration for Nonorthogonal Multiple Access systems (NOMA). These results are valid for NOMA systems and cannot be applied in Orthogonal Multiple Access (OMA) as considered in our paper. In this paper, we derive the harvesting duration that maximizes the throughput. Our contributions are

*Correspondence: nbenhalima@taibahu.edu.sa

- We derive the Cumulative Distribution Function (CDF) of SNR as well as Packet Error Probability (PEP) and throughput. All expressions are valid for Nakagami fading channels. The PEP and throughput are derived in closed form. To the best of our knowledge, these performance metrics were not yet derived in closed form for EH systems in the presence of Nakagami channels.
- We analyze the end-to-end performance for Opportunistic AF (O-AF) and O-DF.
- The suggested optimal harvesting duration allows significant throughput enhancement.
- In [1-22], the analysis is performed at the symbol level. Our results deal with throughput analysis at the packet level. Besides, our derivations are valid for arbitrary positions of source, relay nodes and destination.

Next section describes the network model. Sections 3 and 4 derives the CDF of SNR for O-AF and O-DF. The end-to-end throughput is analyzed in section 5. Theoretical and computer simulations are provided in section 6. Conclusions are presented in last section.

2. Network model

The network model is shown in Figure 1. It contains a source S, L relays R_k and a destination D.

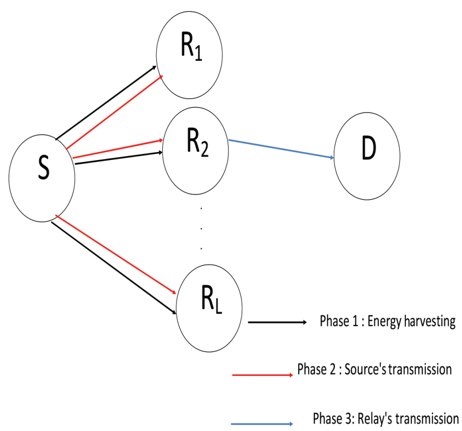

Figure 1. Network model.

The frame with duration T contains in three slots :

- The duration of first time slot is αT. In this first time slot, the relays harvest energy from RF signal received from the source.

  The harvested energy at k-th relay is expressed as [21-24]

$$E_k = \delta\alpha T P_S |g_{SR_k}|^2 = \delta\alpha n_0 E_S |g_{SR_k}|^2, \tag{1}$$

  where $0< \delta < 1$ is the energy conversion efficiency, P_S is the power of S, $E_S = T_s P_S$, T_s is the symbol period, $n_0 = T/T_s$ is the number of symbols per frame and g_{SR_k} is the channel coefficient between S and R_k.

- The duration of second time slot is $(1-\alpha)T/2$. In this second time slot, the source S transmits $n_0(1-\alpha)/2$ symbols to all relays R_k, $k = 1...L$.

The received signal at relay R_k during n-th symbol period is written as

$$y_{R_k}(n) = \sqrt{E_S} g_{SR_k} x(n) + n_{SR_k}(n), 1 \leq n \leq n_0(1-\alpha)/2, \tag{2}$$

where $x(n)$ is the n-th transmitted symbol and $n_{SR_k}(n)$ is a Gaussian noise with variance N_0.

- The duration of third time slot is $(1-\alpha)T/2$.

2.1. AF relaying

In this third time slot, a selected relay amplifies the received signal to the destination D.

The transmit symbol energy of the k-th relay R_k, E_{R_k}, is equal to the harvested energy E_k divided by the number of transmitted symbol during third time slot, $n_0(1-\alpha)/2$. It is expressed as [21]

$$E_{R_k} = \frac{E_k}{n_0(1-\alpha)/2} = \Delta |g_{SR_k}|^2, \tag{3}$$

where

$$\Delta = \frac{2\delta\alpha E_S}{1-\alpha}. \tag{4}$$

The amplification factor of the chosen relay is written as

$$G_k = \sqrt{\frac{E_{R_k}}{N_0 + E_S|g_{SR_k}|^2}} < \sqrt{\frac{E_{R_k}}{E_S|g_{SR_k}|^2}} = \sqrt{\frac{\Delta}{E_S}}. \tag{5}$$

In cooperative systems, the SNR at the relay, $\frac{E_S|g_{SR_k}|^2}{N_0}$, should be high to guarantee a high throughput at destination [25]. Therefore, we can neglect N_0 in (5). This approximation is tight at high SNR.

The relay transmits an amplified version of its received signal equal to $G_k y_{R_k}(n)$. The received signal at D is

$$y_D(n) = g_{R_kD} G_k y_{R_k}(n) + n_D(n), 1 \leq n \leq n_0(1-\alpha)/2. \tag{6}$$

Using (2), we have

$$y_D(n) = \sqrt{E_S} g_{R_kD} g_{SR_k} G_k x(n) + G_k g_{R_kD} n_{SR_k}(n) + n_D(n), 1 \leq n \leq n_0(1-\alpha)/2, \tag{7}$$

where g_{R_kD} is the channel coefficient between R_k and D.

2.2. DF relaying

In the third time slot, a chosen relay detects the source packet containing $(1-\alpha)n_0/2$ symbols and transmit it to the destination. The decision variable used by the relay R_k is expressed as

$$\widetilde{y}_{R_k}(n) = y_{R_k}(n) \times g^*_{SR_k}, \tag{8}$$

where $g^*_{SR_k}$ is the conjugate of g_{SR_k} and $y_{R_k}(n)$ is given in (2).

The decision variable is compared to thresholds of QAM modulation to detect $x(n)$ [26]. Parity bits are used to check if all symbols of the packet were correctly detected. If a relay correctly detected the packet and offers the highest SNR at D, it transmits the detected symbols $\widehat{x}(n), 1 \leq n \leq (1-\alpha)n_0/2$. The received signal at D is written as

$$y_D(n) = \sqrt{E_{R_{sel}}} g_{R_{sel}D} \widehat{x}(n) + n_D(n), \tag{9}$$

where $E_{R_{sel}}$ is the transmitted energy per symbol of selected relay R_{sel} and $g_{R_{sel}D}$ is channel coefficient between R_{sel} and D.

3. CDF of SNR for opportunistic AF relaying

3.1. CDF of SNR for a given relay

Using (7), when the k-th relay is activated, the SNR at D is written as

$$\gamma_{S,R_k,D} = \frac{G_k^2 E_S |g_{SR_k}|^2 |g_{R_kD}|^2}{N_0 + N_0 G_k^2 |g_{R_kD}|^2} = \frac{E_S |g_{SR_k}|^2 |g_{R_kD}|^2}{\frac{N_0}{G_k^2} + N_0 |g_{R_kD}|^2}. \tag{10}$$

Using (5), the SNR can be upper bounded by

$$\gamma_{S,R_k,D} < \gamma_{S,R_k,D}^{up} = \frac{aX_1^{(k)} X_2^{(k)}}{b + cX_2^{(k)}}, \tag{11}$$

where

$$a = E_S, \tag{12}$$

$$b = \frac{N_0 E_S}{\Delta}, \tag{13}$$

$$c = N_0, \tag{14}$$

$$X_1^{(k)} = |g_{SR_k}|^2, \tag{15}$$

$$X_2^{(k)} = |g_{R_kD}|^2. \tag{16}$$

To obtain the upper bound in (11), we replaced G_k by its upper bound $\sqrt{\frac{\Delta}{E_S}}$ given in (5).

Using (5), the SNR can be upper bounded by

$$\gamma_{S,R_k,D}^{up} = \frac{a}{c} \frac{X_1^{(k)} X_2^{(k)}}{D + X_2^{(k)}}, \tag{17}$$

where

$$D = \frac{b}{c} = \frac{E_S}{\Delta} = \frac{1-\alpha}{2\delta\alpha}. \tag{18}$$

The CDF of $\gamma_{D,k}^{up}$ is equal to

$$F_{\gamma_{S,R_k,D}^{up}}(x) = \int_0^{+\infty} P\left(\frac{X_1^{(k)} y}{D + y} \leq \frac{xc}{a}\right) f_{X_2^{(k)}}(y) dy, \tag{19}$$

where $f_{X_2^{(k)}}(y)$ is the Probability Density Function (PDF) of $X_2^{(k)}$ written as

$$f_{X_2^{(k)}}(y) = \frac{m_{2,k}^{m_{2,k}} y^{m_{2,k}-1}}{\lambda_{2,k}^{m_{2,k}} \Gamma(m_{2,k})} e^{-\frac{m_{2,k} y}{\lambda_{2,k}}}, \tag{20}$$

where $m_{i,k}$ is the fading figure of Nakagami channel describing the statistics of $X_i^{(k)}$, $\lambda_{i,k} = E(X_i^{(k)})$ for i=1,2, $E(.)$ is the expectation operator. We have

$$P(\frac{X_1^{(k)} y}{D+y} \leq \frac{xc}{a}) = F_{X_1^{(k)}}(\frac{xc(D+y)}{ay}), \tag{21}$$

where $F_{X_1^{(k)}}(u)$ is the CDF of $X_1^{(k)}$ written as

$$F_{X_1^{(k)}}(u) = 1 - \frac{\Gamma(m_{1,k}, \frac{m_{1,k} u}{\lambda_{1,k}})}{\Gamma(m_{1,k})}, \tag{22}$$

where $\Gamma(.,.)$ is the incomplete Gamma function.

Using (19), (21) and (22), we obtain

$$F_{\gamma_{S,R_k,D}^{up}}(x) = 1 - \frac{m_{2,k}^{m_{2,k}}}{\lambda_{2,k}^{m_{2,k}} \Gamma(m_{2,k}) \Gamma(m_{1,k})} \int_0^{+\infty} y^{m_{2,k}-1} e^{-\frac{m_{2,k} y}{\lambda_{2,k}}} \Gamma(m_{1,k}, \frac{m_{1,k} xc(D+y)}{ay\lambda_{1,k}}) dy. \tag{23}$$

Using [27] equation 8.352.2, we have

$$\Gamma(n,x) = (n-1)! e^{-x} \sum_{q=0}^{n-1} \frac{x^q}{q!}. \tag{24}$$

Let $E = \frac{m_{1,k} xc}{a\lambda_{1,k}}$, using (24), the last term of (23) is expressed as

$$\Gamma(m_{1,k}, \frac{m_{1,k} xc(D+y)}{ay\lambda_{1,k}}) = \Gamma(m_{1,k}, \frac{E(D+y)}{y}) = (m_{1,k}-1)! e^{-E-\frac{ED}{y}} \sum_{q=0}^{m_{1,k}-1} \frac{E^q y^{-q} (D+y)^q}{q!}. \tag{25}$$

We deduce

$$\Gamma(m_{1,k}, \frac{m_{1,k} xc(D+y)}{ay\lambda_{1,k}}) = (m_{1,k}-1)! e^{-E-\frac{ED}{y}} \sum_{q=0}^{m_{1,k}-1} \frac{E^q y^{-q}}{q!} \sum_{l=0}^{q} \binom{q}{l} D^{q-l} y^l. \tag{26}$$

Using (23) and (26), we have

$$F_{\gamma_{S,R_k,D}^{up}}(x) = 1 - \frac{e^{-E} m_{2,k}^{m_{2,k}} (m_{1,k}-1)!}{\lambda_{2,k}^{m_{2,k}} \Gamma(m_{2,k}) \Gamma(m_{1,k})} \sum_{q=0}^{m_{1,k}-1} \frac{E^q}{q!} \sum_{l=0}^{q} \binom{q}{l} D^{q-l} \int_0^{+\infty} y^{l+m_{2,k}-1-q} e^{-\frac{m_{2,k} y}{\lambda_{2,k}}} e^{-\frac{ED}{y}} dy. \tag{27}$$

Using [27] equation 3.471.9, we have

$$\int_0^{+\infty} x^{n-1} e^{-\frac{a}{y}} e^{-by} dy = 2(\frac{a}{b})^{\frac{n}{2}} K_n(2\sqrt{ab}). \tag{28}$$

Using (28), (27) is expressed as

$$F_{\gamma^{up}_{S,R_k,D}}(x) = 1 - 2\frac{e^{-E} m_{2,k}^{m_{2,k}}(m_{1,k}-1)!}{\lambda_{2,k}^{m_{2,k}}\Gamma(m_{2,k})\Gamma(m_{1,k})}\sum_{q=0}^{m_{1,k}-1}\frac{E^q}{q!}\sum_{l=0}^{q}\binom{q}{l}D^{q-l}\left(\frac{ED\lambda_{2,k}}{m_{2,k}}\right)^{\frac{l+m_{2,k}-q}{2}}K_{l+m_{2,k}-q}\left(2\sqrt{ED\frac{m_{2,k}}{\lambda_{2,k}}}\right). \tag{29}$$

Using the expression of E, we obtain

$$F_{\gamma^{up}_{S,R_k,D}}(x) = 1 - 2\frac{e^{-\frac{m_{1,k}xc}{a\lambda_{1,k}}} m_{2,k}^{m_{2,k}}(m_{1,k}-1)!}{\lambda_{2,k}^{m_{2,k}}\Gamma(m_{2,k})\Gamma(m_{1,k})}\sum_{q=0}^{m_{1,k}-1}\frac{\left(\frac{m_{1,k}xc}{a\lambda_{1,k}}\right)^q}{q!}\sum_{l=0}^{q}\binom{q}{l}D^{q-l}\left(\frac{m_{1,k}xcD\lambda_{2,k}}{a\lambda_{1,k}m_{2,k}}\right)^{\frac{l+m_{2,k}-q}{2}},$$

$$K_{l+m_{2,k}-q}\left(2\sqrt{m_{1,k}xcD\frac{m_{2,k}}{a\lambda_{1,k}\lambda_{2,k}}}\right). \tag{30}$$

The last expression is used to obtain a lower bound of CDF of SNR as follows:

$$F_{\gamma_{S,R_k,D}}(x) > F_{\gamma^{up}_{S,R_k,D}}(x). \tag{31}$$

3.2. CDF of SNR for the selected relay

When there are L available relays, we can select the relay with the highest SNR known as Opportunistic AF (O-AF), the corresponding SNR is expressed as

$$\gamma_{S,R_{sel},D} = \max_{1\leq k\leq L}\gamma_{S,R_k,D}, \tag{32}$$

where R_{sel} is the selected relay.

If $\gamma_{S,R_k,D}$ are independent, we have

$$F_{\gamma_{S,R_{sel},D}}(x) = \prod_{k=1}^{L}F_{\gamma_{S,R_k,D}}(x) > \prod_{k=1}^{L}F_{\gamma^{up}_{S,R_k,D}}(x), \tag{33}$$

where $F_{\gamma^{up}_{S,R_k,D}}(x)$ is given in (30).

An upper bound of PEP of AF relaying is deduced from the CDF of SNR [28],

$$PEP < F_{\gamma_{S,R_{sel},D}}(s_0). \tag{34}$$

s_0 is waterfall threshold defined as [28]

$$s_0 = \int_0^{+\infty} h(x)dx. \tag{35}$$

$h(x)$ is the PEP for SNR equal x written as

$$h(x) = 1 - [1 - SEP(x)]^N. \tag{36}$$

This equation gives the PEP for Q-QAM and N is the number of symbols per packet. A packet is correctly received if all N symbols are correct. $SEP(x)$ is the Symbol Error Probability of QAM modulation [26]

$$SEP(x) = 2\left(1 - \frac{1}{\sqrt{Q}}\right) erfc\left(\sqrt{x\frac{3\log_2(Q)}{2(Q-1)}}\right). \tag{37}$$

4. Performance analysis of opportunistic DF

4.1. PEP of O-DF

In O-DF, the chosen relay should have correctly decoded the source packet. Also, this relay has the largest SNR at D among the relays that have correctly decoded the source packet. The PEP of O-DF is written as

$$PEP = \sum_{u\in\{1,\ldots,L\}} P(u)PEP(u). \tag{38}$$

$P(u)$ is the probability that only relays in set u correctly detected the source packet :

$$P(u) = \prod_{j\in u}(1 - PEP_j)\prod_{k\notin u} PEP_k. \tag{39}$$

PEP_j is the probability at relay R_j and [28]

$$PEP(u) < \prod_{k\in u} F_{\gamma_{R_k D}}(s_0). \tag{40}$$

The SNR at D is the maximum of SNRs between relays that have correctly decoded.

The SNR at j-th relay follows a Gamma distribution with CDF equal to

$$F_{\gamma_{SR_j}}(x) = 1 - \frac{\Gamma(m_{1,j}, \frac{m_{1,j}x}{\beta_j})}{\Gamma(m_{1,j})}, \tag{41}$$

where $\beta_j = \frac{\lambda_{1,j}E_s}{N_0}$ is the average SNR at j-th relay.

The PEP at j-th relay is deduced from the CDF of SNR as follows [28]:

$$PEP_j < F_{\gamma_{SR_j}}(s_0). \tag{42}$$

The SNR at destination is analyzed in next subsection.

4.2. SNR statistics for DF relaying

Using (3), the transmitted energy per symbol of the relay is expressed as

$$E_{R_i} = 2\delta E_S \frac{\alpha}{1-\alpha}|g_{SR_i}|^2. \tag{43}$$

The SNR at the destination D is given by

$$\gamma_{R_i D} = \frac{E_{R_i}}{N_0}|g_{R_i D}|^2 = 2\delta\alpha\frac{E_S}{N_0(1-\alpha)}|g_{SR_i}|^2|g_{R_i D}|^2. \tag{44}$$

For Nakagami fading channels, the SNR is the product of two Gamma random variables (r.v).

Theorem :

Let $X = X_1 X_2$ be the product of two Gamma random variables (r.v) X_1 and X_2. The PDF of X_1 and X_2 is written as

$$f_{X_1}(x) = \frac{x^{\alpha_1 - 1} e^{-\frac{x}{\beta_1}}}{\Gamma(\alpha_1)\beta_1^{\alpha_1}}, x \geq 0, \tag{45}$$

$$f_{X_2}(x) = \frac{x^{\alpha_2 - 1} e^{-\frac{x}{\beta_2}}}{\Gamma(\alpha_2)\beta_2^{\alpha_2}}, x \geq 0. \tag{46}$$

The PDF of X is given by [29]

$$f_X(x) = 2\left(\frac{x}{\beta_1\beta_2}\right)^{\frac{\alpha_1+\alpha_2}{2}} \frac{K_{\alpha_2-\alpha_1}\left(2\sqrt{\frac{x}{\beta_1\beta_2}}\right)}{x\Gamma(\alpha_1)\Gamma(\alpha_2)}. \tag{47}$$

We deduce the CDF of X :

$$F_X(x) = \int_0^x 2\left(\frac{u}{\beta_1\beta_2}\right)^{\frac{\alpha_1+\alpha_2}{2}} \frac{K_{\alpha_2-\alpha_1}\left(2\sqrt{\frac{u}{\beta_1\beta_2}}\right)}{u\Gamma(\alpha_1)\Gamma(\alpha_2)} du. \tag{48}$$

Let $v = 2\sqrt{\frac{u}{\beta_1\beta_2}}$ so that $u = \frac{\beta_1\beta_2 v^2}{4}$ and $du = \frac{\beta_1\beta_2}{2} v dv$. We have

$$\begin{aligned} F_X(x) &= \frac{2^{2-\alpha_1-\alpha_2}}{\Gamma(\alpha_1)\Gamma(\alpha_2)} \int_0^{2\sqrt{\frac{x}{\beta_1\beta_2}}} v^{\alpha_1+\alpha_2-1} K_{\alpha_2-\alpha_1}(v)\, dv \\ &= \frac{2^{2-\alpha_1-\alpha_2}}{\Gamma(\alpha_1)\Gamma(\alpha_2)} A_{\alpha_1+\alpha_2-1,\alpha_2-\alpha_1}(2\sqrt{\frac{x}{\beta_1\beta_2}}), \end{aligned} \tag{49}$$

where

$$A_{x,y}(x) = \int_0^x u^x K_y(u) du \tag{50}$$

X_1 and X_2 are defined as

$$X_1 = |g_{SR_i}|^2, \tag{51}$$

and

$$X_2 = |g_{R_iD}|^2. \tag{52}$$

The PDF of X, X_1 and X_2 are given in (49), (45) and (46) with $\alpha_1 = m_{1,i}$, $\beta_1 = \frac{\lambda_{SR_i}}{m_{1,i}}$, $\alpha_2 = m_{2,i}$, $\beta_2 = \frac{\lambda_{R_iD}}{m_{2,i}}$ with

$$\lambda_{XY} = E(|g_{XY}|^2). \tag{53}$$

The SNR D is written as

$$\gamma_{R_iD} = \frac{2\delta\alpha E_S}{(1-\alpha)N_0}|g_{SR_i}|^2|g_{R_iD}|^2 = \frac{2\delta\alpha E_S}{(1-\alpha)N_0}X. \tag{54}$$

The CDF and PDF of SNR of link $R_i - D$ can be deduced from the statistics of X as follows:

$$\begin{aligned} F_{\gamma_{R_iD}}(x) &= F_X(x\frac{(1-\alpha)N_0}{2\delta\alpha E_S}) = \frac{2^{2-\alpha_1-\alpha_2}}{\Gamma(\alpha_1)\Gamma(\alpha_2)}A_{\alpha_1+\alpha_2-1,\alpha_2-\alpha_1}(2\sqrt{\frac{(1-\alpha)N_0x}{2\delta\alpha E_S\beta_1\beta_2}}) \\ &= \frac{2^{2-m_{1,i}-m_{2,i}}}{\Gamma(m_{1,i})\Gamma(m_{2,i})}A_{m_{1,i}+m_{2,i}-1,m_{2,i}-m_{1,i}}(2\sqrt{\frac{(1-\alpha)N_0xm_{1,i}m_{2,i}}{2\delta\alpha E_S\lambda_{R_iD}\lambda_{SR_i}}}), \end{aligned} \tag{55}$$

$$\begin{aligned} f_{\gamma_{R_iD}}(x) &= \frac{(1-\alpha)N_0}{2\delta\alpha E_S}p_X(x\frac{(1-\alpha)N_0}{2\delta\alpha E_S}) \\ &= 2\left(\frac{(1-\alpha)N_0}{2\delta\alpha E_S}x\right)^{\frac{\alpha_1+\alpha_2}{2}-1}(\beta_1\beta_2)^{-\alpha_1/2-\alpha_2/2}\frac{(1-\alpha)N_0}{2\delta\alpha E_S}\frac{K_{\alpha_2-\alpha_1}\left(2\sqrt{\frac{x(1-\alpha)N_0}{\beta_1\beta_2 2\delta\alpha E_S}}\right)}{\Gamma(\alpha_1)\Gamma(\alpha_2)} \end{aligned}$$

$$= 2\left(\frac{x(1-\alpha)N_0}{2\delta\alpha E_S}\right)^{\frac{m_{1,i}+m_{2,i}}{2}-1}(\frac{\lambda_{R_iD}\lambda_{SR_i}}{m_{1,i}m_{2,i}})^{-m_{1,i}/2-m_{2,i}/2}\frac{(1-\alpha)N_0}{2\delta\alpha E_S}\frac{K_{m_{2,i}-m_{1,i}}\left(2\sqrt{\frac{m_{1,i}m_{2,i}x(1-\alpha)N_0}{2\delta\alpha E_S\lambda_{R_iD}\lambda_{SR_i}}}\right)}{\Gamma(m_{1,i})\Gamma(m_{2,i})}. \tag{56}$$

5. Throughput analysis and optimization

The throughput is the number of correctly received bits divided by time duration and used bandwidth B:

$$Thr(\alpha) = \frac{(1-\alpha)log_2(Q)n_0(1-PEP)}{2TB} = \frac{(1-\alpha)}{2}log_2(Q)(1-PEP), \tag{57}$$

where Q is the size of the modulation, $T = n_0T_s$ and $B = 1/T_s$ is the bandwidth. The PEP is deduced from the CDF of SNR using (34) or (38) for AF and DF relaying.

For large values of α, the harvested energy is large so that the PEP decreases but the throughput is small since it is proportional to $1-\alpha$. For small values of α, the available time for transmission $(1-\alpha)T$ increases but the PEP is high since the harvested energy is low, so that the throughput is low. The value of α is optimized to enhance the throughput

$$\alpha_{opt} = argmax_{\alpha}Thr(\alpha). \tag{58}$$

The optimal α_{opt} is obtained as follows:

Initialization

$\alpha_A = 0.001$

$\alpha_B = 0.002$

- Iterations

While $Thr(\alpha_B) > Thr(\alpha_A)$
$\alpha_A = \alpha_B$
$\alpha_B = \alpha_B + 0.001$
end
The optimal harvesting duration is expressed as $\alpha_{opt} = (\alpha_A + \alpha_B)/2$.

The derivative of throughput with respect to α is given in Appendix A. We studied a network containing a single relay and suggested the use of Newton search algorithm to find the optimal harvesting duration.

6. Theoretical and simulation results

Simulation and theoretical curves were plotted with MATLAB for packet length equal to 200 symbols and energy conversion efficiency $\delta = 0.5$. We set the fading figure as follows : $m_{SR_k} = m_1$ and $m_{R_kD} = m_2$. Except figure 6, we set $m_1 = 2$ and $m_2 = 3$. A 64-QAM modulation was used during the simulations.

Figure 2 shows the throughput of O-AF in presence of L=2,3 and 4 relays. We notice that the throughput improves as L increases due to cooperative diversity. Computer simulations are close to theoretical curves and we conclude that our derivations are correct.

Figure 3 shows the throughput of O-AF versus harvesting duration. We notice that the throughput can be maximized by selecting the harvesting duration. When α increases, the PEP decreases as the harvested energy increases since the duration of energy harvesting slot is α T. However, if we choose a very large value for α, there is no sufficient time to transmit symbols by the source and relays as the duration of second slot is $(1-\alpha)$T/2. Also, if α is very small, we can transmit more data in second and third slots but the harvested energy is very low. Therefore, harvesting duration must be optimized to make a compromise between harvesting and data transmission durations. Figure 4 shows the throughput for optimal α with respect to $\alpha = 1/3$ [1-21]. For $\alpha = 1/3$, the same duration is allocated to EH, S and relay transmission as suggested in [1-21]. The proposed optimal harvesting duration allows significant throughput enhancement. The optimal harvesting duration versus average SNR per bit is shown in Figure 5. We observe that harvesting duration can be reduced at high SNR.

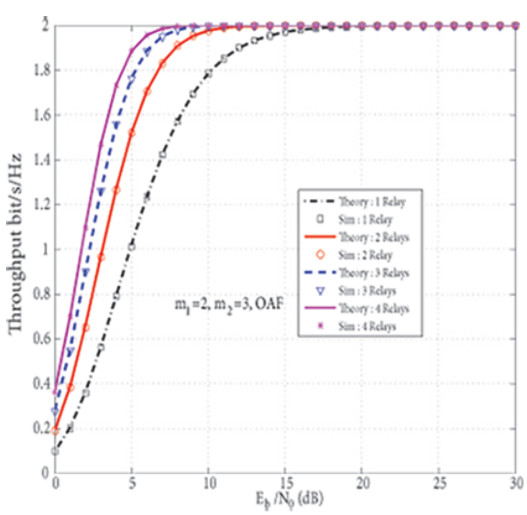

Figure 2. Throughput of O-AF for $\alpha = 1/3$.

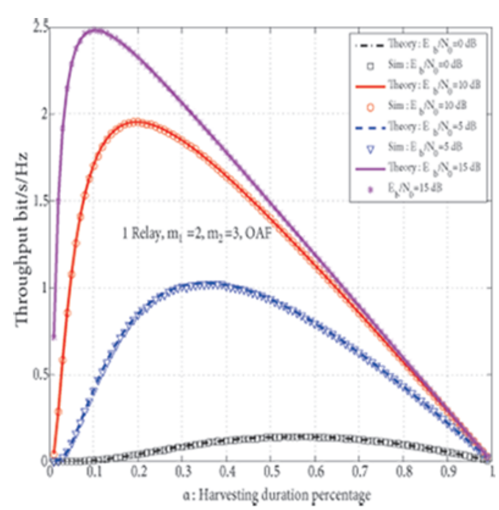

Figure 3. Throughput of O-AF versus harvesting duration percentage α.

Figure 6 shows the throughput of O-AF for Rayleigh and Nakagami fading channels. We notice that the throughput increases as the fading parameter m_{XY} increases. A good accordance between theoretical and simulation results confirm the accuracy of our derivation for both Rayleigh $m_{XY} = 1$ and Nakagami channels.

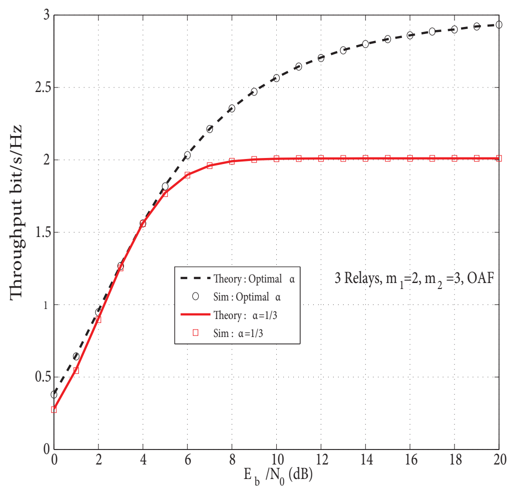

Figure 4. Throughput of O-AF for optimal harvesting duration and $\alpha = 1/3$.

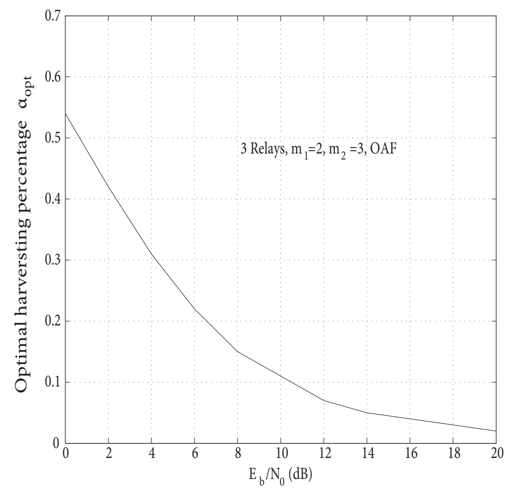

Figure 5. Optimal Harvesting Duration for O-AF.

Figure 7 shows the throughput of O-DF for Nakagami channels. The throughput improves as the number of relays increases due to cooperative diversity. Figure 8 shows that we can optimized harvesting duration for O-DF. These results were obtained for a network containing three relays. Harvesting duration should be increased (respectively decreased) at low (respectively high) SNR. Figure 9 shows that the proposed optimal harvesting duration allows significant throughput enhancement with respect to $\alpha = 1/3$ [1-21]. The suggested optimal harvesting duration is plotted in Figure 10 with respect to average SNR per bit. Figure 10 corresponds to O-DF relaying.

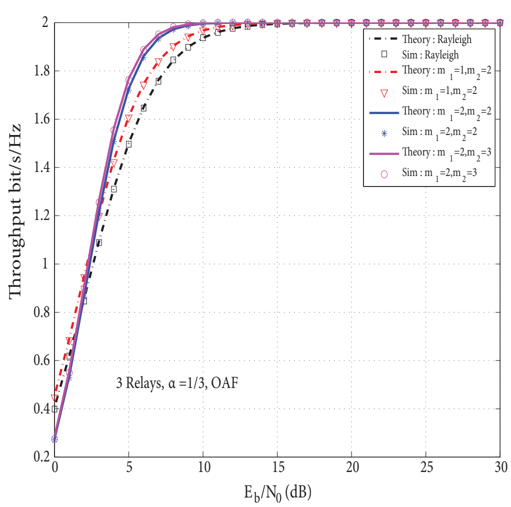

Figure 6. Throughput of O-AF for Nakagami and Rayleigh fading channels.

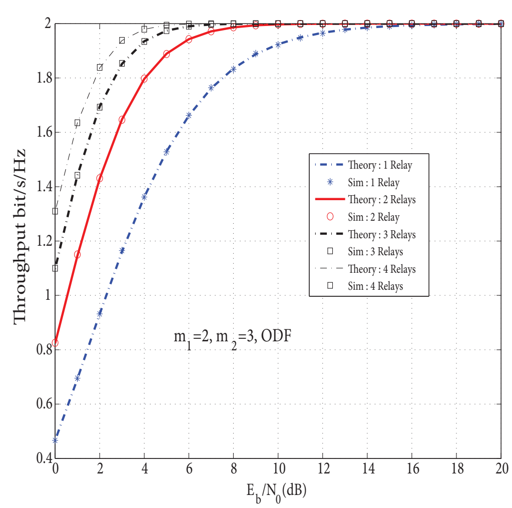

Figure 7. Throughput of O-DF for $\alpha = 1/3$ and different number of relays.

Figure 11 compares the throughput of energy harvesting systems to non energy harvesting. We studied OAF with three relays for $m_1 = 2$ and $m_2 = 3$ and 64 QAM modulation. Nonenergy harvesting offers a higher throughput than energy harvesting with optimal harvesting duration. However, the battery of non energy harvesting systems should be recharged or replaced. For example, Wireless Sensor Networks (WSN) with energy harvesting has an unlimited lifetime. WSN without energy harvesting capabilities require to recharge or change the battery which may not be easily performed.

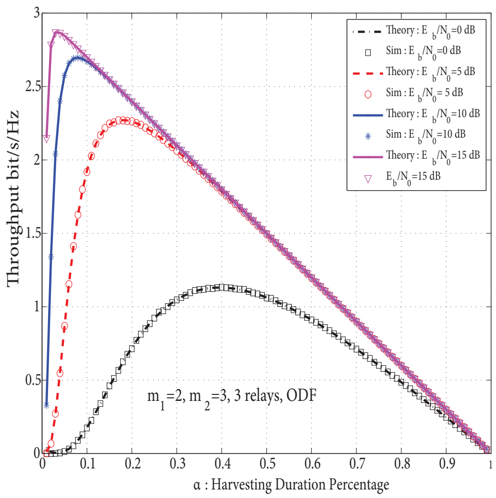

Figure 8. Optimal harvesting duration versus E_b/N_0 for O-DF.

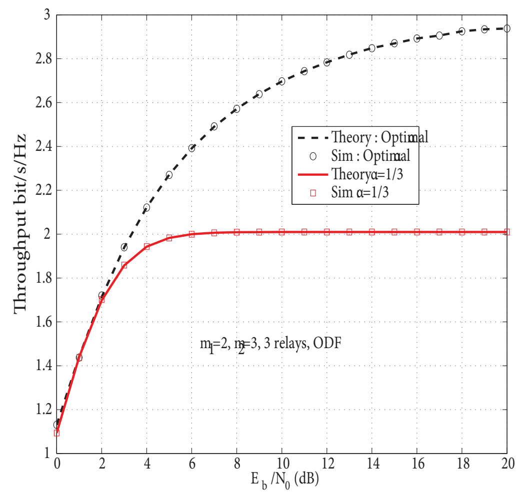

Figure 9. Throughput of O-DF for $\alpha = 1/3$ and optimal harvesting duration.

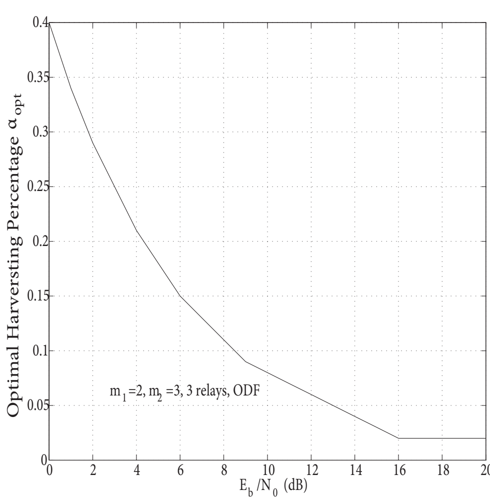

Figure 10. Optimal harvesting duration versus E_b/N_0 for O-DF.

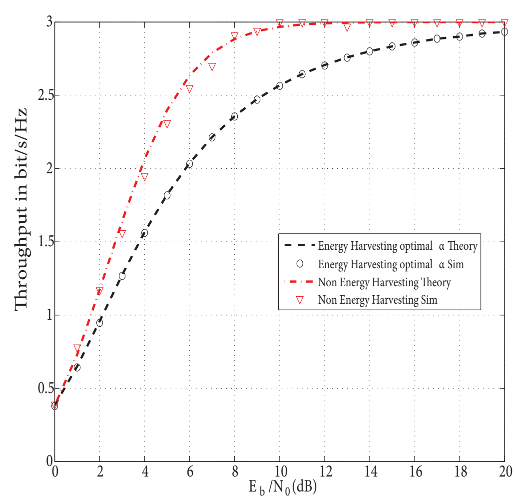

Figure 11. Throughput comparison of energy harvesting and non energy harvesting for AF relaying and 64 QAM modulation.

7. Conclusions

In this paper, we have studied the performance of cooperative systems where the relays harvest energy from RF signal received from the source. We have suggested to optimize harvesting duration to reach higher data rates. In previous studies, harvesting duration has not been yet optimized. Our results are valid for O-AF and O-DF in the presence of Nakagami fading channels. The throughput and packet error probability were derived in closed form.

References

[1] Zhan J, Liu Y, Tang X, Chen Q. Relaying protocols for buffer-aided energy harvesting wireless cooperative networks. IET Networks 2018; 7: 109 - 118.

[2] Xiuping W, Feng Y, Tian Z. The DF-AF Selection relay transmission based on energy harvesting. In: 2018 10th International Conference on Measuring Technology and Mechatronics Automation (ICMTMA); Montreal, Canada; 2018. pp. 174 - 177.

[3] Nguyen HT, Nguyen SQ, Hwang WJ. Outage probability of energy harvesting relay systems under unreliable backhaul connections. In: 2018 2nd International Conference on Recent Advances in Signal Processing, Telecommunications and Computing (SigTelCom); Akihabara, Vietnam; 2018. pp. 19-23.

[4] Qiu C, Hu Y, Chen Y. Lyapunov Optimized Cooperative Communications With Stochastic Energy Harvesting Relay. IEEE Internet of Things Journal 2018; 5: 1323-1333.

[5] Sui D, Hu F, Zhou W, Shao M, Chen M. Relay selection for radio frequency energy-harvesting wireless body area network with buffer. IEEE Internet of Things Journal 2018; 5: 1100-1107.

[6] Dung LT, Hoang TM, Tan NT, Choi SG. Analysis of partial relay selection in NOMA systems with RF energy harvesting.In: 2018 2nd International Conference on Recent Advances in Signal Processing, Telecommunications and Computing (SigTelCom); Akihabara, Vietnam; 2018. pp. 13-18.

[7] Le QN, Bao VNQ, An B. Full-duplex distributed switch-and-stay energy harvesting selection relaying networks with imperfect CSI: Design and outage analysis. Journal of Communications and Networks 2018; 20: 29-46.

[8] Chiu HC, Huang WJ. Precoding design in two-way cooperative system with energy harvesting relay.In: 2018 27th Wireless and Optical Communication Conference (WOCC); Hualien, Taiwan; 2018. pp. 1-5.

[9] Gurjar DS, Singh U, Upadhyay PK. Energy harvesting in hybrid two-way relaying with direct link under Nakagami-m fading. In: 2018 IEEE Wireless Communications and Networking Conference (WCNC); Barcelona, Spain; 2018. pp. 1-6.

[10] Singh K, Ku ML, Lin JC, Ratnarajah T. Toward optimal power control and transfer for energy harvesting amplify-and-forward relay networks. IEEE Transactions on Wireless Communications 2018; 17: 4971-4986.

[11] Wu Y, Qian LP, Huang L, Shen X. Optimal relay selection and power control for energy-harvesting wireless relay networks. IEEE Transactions on Green Communications and Networking 2018; 2: 471 - 481.

[12] Fan R, Atapattu S, Chen W, Zhang Y, Evans J. Throughput maximization for multi-hop decode-and-forward relay network with wireless energy harvesting. IEEE Access 2018; 6: 24582-24595.

[13] Huang Y, Wang J, Zhang P, Wu Q. Performance analysis of energy harvesting multi-antenna relay networks with different antenna selection schemes. IEEE Access 2017; 6: 5654-5665.

[14] Babaei M, Aygolu U, Basar E, BER Analysis of dual-hop relaying with energy harvesting in nakagami-m fading channel. IEEE Transactions on Wireless Communications 2018; 17: 4352 - 4361.

[15] Kalluri T, Peer M, Bohara VA, Dacosta DB, Dias US. Cooperative spectrum sharing-based relaying protocols with wireless energy harvesting cognitive user. IET Communications 2018; 7: 838 - 847.

[16] Xie D, Lai X, Lei X, Fan L. Cognitive multiuser energy harvesting decode-and-forward relaying system with direct links. IEEE Access 2018; 6: 5596-5606.

[17] Yan Z, Chen S, Zhang X, Liu HL. Outage performance analysis of wireless energy harvesting relay-assisted random underlay cognitive networks. IEEE Internet of Things Journal 2018; 5: 2691-2699.

[18] Vo VN, Nguyen TG, In CS, Baig ZA, Sanguanpong S. Secrecy outage performance analysis for energy harvesting sensor networks with a jammer using relay selection strategy. IEEE Access 2018; 6: 23406-23419.

[19] Yao R, Lu Y, Tsiftsis AT, Qi N, Mekkawy T et al. Secrecy rate-optimum energy splitting for an untrusted and energy harvesting relay network. IEEE Access 2018; 6: 19238-19246.

[20] Yin C, Nguyen HT, Kundu C, Kaleem Z, Palacios EG, Duong TQ. Secure energy harvesting relay networks with unreliable backhaul connections. IEEE Access 2018; 6: 12074 - 12084.

[21] Lei H, Xu M, Ansari IS, Pan G, Qaraqe KA, Alouini MS. On secure underlay mimo cognitive radio networks with energy harvesting and transmit antenna selection. IEEE Transactions on Green Communications and Networking 2017; 1: 192-203.

[22] Hoang TM, Son VV, Dinh NC, Hiep PT. Optimizing duration of energy harvesting for downlink NOMA full-duplex over Nakagami-m fading channel. AEU - International Journal of Electronics and Communications 2018; 95: 199-206.

[23] Mishra D, Swades D. Optimal time allocation for rf-powered df relay- assisted cooperative communication. Electronics Letters 2016; 52: 1274 - 1276.

[24] Nasir AA, Zhou X, Durrani S, Kennedy RA. Relaying protocols for wireless energy harvesting and information processing. IEEE Transactions on Wireless Communications 2013; 12: 3622-3636.

[25] Anghel PA, Kaveh M. Exact symbol error probability of a cooperative network in a Rayleigh fading environnement. IEEE Transition on Wireless Communication 2004; 3: 1416-1421.

[26] Proakis J. Digital Communications. New York: Mac Graw-Hill, 2007.

[27] Gradshteyn IS, Ryzhik IM. Table of Integrals, Series and Products. San Diego, CA: Academic, 1994.

[28] Xi Y, Burr A, Wei JB, Grace D. A General upper bound to evaluate packet error rate over quasi-static fading channels. IEEE Trans. Wireless Communications 2011; 10: 1373-1377.

[29] Withers CS, Nadarajah S. On the product of gamma random variables. Quality and Quantity 2013; 47: 545-552.

Appendix: Derivative of throughput with respect to harvesting duration α

In the presence of a single AF relay, the throughput is lower bounded

$$Thr(\alpha) > Thr_{low}(\alpha) = \frac{1-\alpha}{2} log_2(Q)[1 - F_{\gamma_{SRD}}(s_0)], \tag{59}$$

where $F_{\gamma_{SRD}}(s_0)$ given in (30) depends on α since coefficient $D = \frac{1-\alpha}{2\delta\alpha}$ (18).

The optimal α verifies

$$\frac{\partial Thr_{low}(\alpha)}{\partial\alpha} = A(\alpha) = \frac{-log_2(Q)}{2}[1 - F_{\gamma_{SRD}}(s_0)] - \frac{1-\alpha}{2} log_2(Q) \frac{\partial F_{\gamma_{SRD}}(s_0)}{\partial\alpha} = 0, \tag{60}$$

where

$$\frac{\partial F_{\gamma_{SRD}}(s_0)}{\partial\alpha} = \frac{-2e^{\frac{-m_{1,k}s_0c}{a\lambda_{1,k}}} m_{2,k}^{m_{2,k}}(m_{1,k}-1)!}{\lambda_{2,k}^{m_{2,k}}\Gamma(m_{2,k})\Gamma(m_{1,k})} \sum_{q=0}^{m_{1,k}-1} \frac{(\frac{m_{1,k}s_0c}{a\lambda_{1,k}})^q}{q!} \sum_{l=0}^{q} \binom{q}{l} \left(\frac{m_{1,k}s_0c\lambda_{2,k}}{a\lambda_{1,k}m_{2,k}}\right)^{\frac{l+m_{2,k}-q}{2}}$$

$$[-(\frac{1-\alpha}{2\delta\alpha})^{\frac{q-l+m_{2,k}-2}{2}}(\frac{q-l+m_{2,k}}{2})(\frac{1}{2\delta\alpha^2})K_{l+m_{2,k}-q}(2\sqrt{\frac{m_{1,k}s_0c(1-\alpha)m_{2,k}}{2\delta\alpha a\lambda_{1,k}\lambda_{2,k}}})$$

$$+\sqrt{\frac{\alpha}{1-\alpha}}\sqrt{\frac{m_{1,k}s_0cm_{2,k}}{2\delta a\lambda_{1,k}\lambda_{2,k}}}K'_{l+m_{2,k}-q}(2\sqrt{\frac{m_{1,k}s_0c(1-\alpha)m_{2,k}}{2\delta\alpha a\lambda_{1,k}\lambda_{2,k}}})]. \tag{61}$$

Optimal harvesting duration can not be obtained in closed form and we can use the Newton search algorithm to optimize α:

$$\alpha_{i+1} = \alpha_i - \frac{A(\alpha_i)}{A'(\alpha_i)}, i = 1, 2, 3, ... \tag{62}$$

Only few iterations are needed to find the optimal value and there is no problem of local maximum as the throughput shown in Figure 3 is concave.